Bioorganic & Medicinal Chemistry 21 (2013) 2975–2987

Contents lists available at SciVerse ScienceDirect

Bioorganic & Medicinal Chemistry

journal homepage: www.elsevier.com/locate/bmc

Development of cell-active non-peptidyl inhibitors of cysteine cathepsins

Dibyendu Dana [a], Anibal R. Davalos [a], Shatarupa De [a], Pratikkumar Rathod [a,b], Ranjith K. Gamage [a], Juliana Huestis [a], Nisar Afzal [a], Yuriy Zavlanov [a], Suneeta S. Paroly [a], Susan A. Rotenberg [a], Gopal Subramaniam [a], Kevin J. Mark [b], Emmanuel J. Chang [b], Sanjai Kumar [a,*]

[a] Department of Chemistry and Biochemistry, Queens College and the Graduate Center of The City University of New York, Queens, NY 11367-1597, USA
[b] Department of Chemistry, York College of The City University of New York, Jamaica, NY 11451, USA

ARTICLE INFO

Article history:
Received 16 January 2013
Revised 15 March 2013
Accepted 23 March 2013
Available online 2 April 2013

Keywords:
Cysteine protease inhibitor
Cathepsin inhibitor
Sulfonyloxiranes
Cancer metastasis
Cell migration

ABSTRACT

Cysteine cathepsins are an important class of enzymes that coordinate a variety of important cellular processes, and are implicated in various types of human diseases. However, small molecule inhibitors that are cell-permeable and non-peptidyl in nature are scarcely available. Herein the synthesis and development of sulfonyloxiranes as covalent inhibitors of cysteine cathepsins are reported. From a library of compounds, compound **5** is identified as a selective inhibitor of cysteine cathepsins. Live cell imaging and immunocytochemistry of metastatic human breast carcinoma MDA-MB-231 cells document the efficacy of compound **5** in inhibiting cysteine cathepsin activity in living cells. A cell-motility assay demonstrates that compound **5** is effective in mitigating the cell-migratory potential of highly metastatic breast carcinoma MDA-MB-231 cells.

1. Introduction

Precisely controlled proteolysis of cellular and extracellular proteins is a critically important cellular event that is elegantly orchestrated by a large family of 561 human proteases.[1] Among these are the fifteen members of cathepsin proteases that are primarily housed in membrane-bound organelles called lysosomes. Members of the cathepsin family, classified in terms of their catalytic nucleophilic residue, consist of 11 cysteine proteases (cathepsin B, C/J/dipeptidyl peptidase I, F, H, L, K, O, S, W, V and Z/X/P), two serine proteases (cathepsin A and G), and two aspartyl proteases (cathepsin D and E).[2] Recent decades of research strongly suggest that cysteine cathepsins play critically important and non-redundant roles in many physiological processes, such as cell death, the immune response, collagen degradation, and neurobiology.[3,4] Furthermore, either gain or loss of function as a result of their mis-regulation has been directly associated with a variety of human pathologies, such as cancer, osteoporosis, and autoimmune and metabolic disorders.[5–8] In addition to their importance in human biology, cysteine cathepsins are also implicated in many other types of diseases involving lower organisms such as parasites.[9,10] Consequently, they are important therapeutic targets for drug development.

It is now well established that over-expression and aberrantly regulated activity of cysteine cathepsins play a major role in promoting many hallmarks of cancer.[5,11] The expression of cysteine cathepsins (e.g., B, F, and L) has indeed been found to be significantly upregulated in solid tumors from various origins, such as breast, skin, colorectal, pancreatic, ovarian, brain, head and neck.[11,12] More importantly, a well-defined role for cysteine cathepsins in promoting cell invasion and cancer metastasis has recently emerged.[13,14] Indeed high level expression of cysteine cathepsin B was observed in invasive tumor cells derived from metastatic cancer patients of distinct origins.[15,16] Deletion of either cysteine cathepsins, B, L or S led to decreased tumor invasion with tumors progressively returning to a more benign form.[12] In a separate study, cysteine cathepsin X was able to compensate in part for the absence of cathepsin B in a mouse model of mammary cancer.[13] In this study, inhibition of cysteine cathepsin X with a neutralizing antibody resulted in a drastic loss of invasive behavior in cathepsin B null cultured cells. E-cadherin, an important adherens junction protein that maintains cell–cell adhesion in epithelial cells, was recently identified as a direct proteolytic target of cysteine cathepsins B, L and S.[12] Since it is well established that functional loss of E-cadherin promotes cell invasion and metastatic behavior of cancer cells, an effective inhibition of this family of enzymes is anticipated to provide significant therapeutic benefit in reducing metastatic potential of solid tumors.[17] These studies have led to an interesting hypothesis that promotes a

* Corresponding author. Tel.: +1 718 997 4120; fax: +1 718 997 5531.
E-mail address: Sanjai.Kumar@qc.cuny.edu (S. Kumar).

0968-0896/$ - see front matter © 2013 Elsevier Ltd. All rights reserved.
http://dx.doi.org/10.1016/j.bmc.2013.03.062

poly-pharmacological approach to target pro-tumorigenic members of cysteine cathepsins collectively for the development of effective anti-cancer agents.

While numerous studies of cysteine cathepsins have clearly established them as important therapeutic targets for the development of anti-cancer agents, progress towards development of small molecule inhibitory agents that are non-peptidyl in nature remains slow. Currently, a majority of the reported inhibitory agents of cysteine cathepsins are peptidyl or peptidomimetic in nature, making them poorly cell permeable (reviewed by Turk et al.).[18] Small molecule inhibitory agents of cysteine cathepsins that are uncharged and non-peptidyl in nature are therefore desirable so that they can be further developed as suitable biological reagents, in addition to serving as lead chemotypes for drug development. Furthermore, if the mechanism of inactivation could be designed to produce a covalent and irreversible chemistry with the catalytic active site Cys residue, then the inhibitors could also be developed as activity-based probes (ABPs) for the functional analysis of cysteine proteases in complex proteomes. Activity-based probes have found extensive applications in functional annotation of enzymes in their native biological environments.[19]

2. Results and discussion

In this study, we synthesized a library of compounds containing sulfonyloxirane moiety in the context of a small non-peptidyl molecule and screened for their efficacy as time-dependent inhibitors of cysteine cathepsins. Compound **5** was identified as the lead inhibitory agent of cysteine cathepsin B. Enzymology and mass spectrometry-based experiments were performed to demonstrate that this class of molecules inhibited cysteine cathepsin B in a covalent and irreversible manner. Importantly, **5** was shown to be effective in inhibiting intracellular activity of cysteine cathepsin B, and the cell migratory behavior of highly metastatic human breast carcinoma MDA-MB-231 cells.

2.1. Design and synthesis of compounds 1–13 and time-dependent inhibitory evaluation

The advent of E-64 from *Aspergillus japonicus*, an epoxysuccinyl-derived inhibitory agent, was a critically important stepping stone for deciphering the undocumented function of cysteine cathepsins family of enzymes.[20] Although, E-64 is a generic non-selective inhibitor of cysteine cathepsins, structural investigation of the E-64-inhibited complex have subsequently led to the development of selective cysteine cathepsin B inhibitors (e.g., CA030 and CA074).[21,22] The marked success of E-64 and its subsequent analogues as effective inhibitors of cysteine cathepsins relies on the exclusive reactivity of an active site cysteine residue with the electrophilic 'warhead' epoxy group. The catalytic mechanism of cysteine cathepsins involves participation of this invariant and reactive cysteine residue.[23] A close visual inspection of the structures of CA030 and CA074 in complex with cysteine cathepsins revealed that there exist well-defined binding pockets, S2 and S1′, surrounding the S1 site (Schechter and Berger nomenclature)[24] that prefer to accommodate aromatic hydrophobic groups.[21,22] It was therefore hypothesized that an arylsulfonyl-substituted oxiranyl moiety could serve as a small molecule covalent inactivator of cysteine cathepsins, targeting the key residues of the core enzyme active site. This approach envisions that (a) an appropriate binding of inhibitory compounds within the active site of cysteine cathepsin will allow the reactive Cys residue to be entrapped by the activated sulfonyloxirane group, (b) the sulfonyl group will likely mimic the potential H-bonding interactions that the carbonyl group α to the epoxy moiety exhibits in the inhibited CA030-cathepsin B complex,[21] and (c) the sulfonyl group will further enhance the electrophilicity of the oxiranyl carbon, compared to a carbonyl group, thereby facilitating the entrapment of the active site Cys residue. Upon successful demonstration of the aforementioned hypotheses, this class of molecules could serve as a new type of chemical motif on which selective cysteine cathepsin inhibitors could be developed in future, exploiting the surrounding S3 and S′ pockets. Such a strategy has indeed been utilized to develop potent and selective inhibitors of cysteine cathepsins.[25–30]

A small library of sulfonyloxirane compounds was therefore synthesized. Cysteine cathepsin B, a promoter of cancer metastasis, was chosen as the initial inhibitory target to evaluate the efficacy by following a time-dependent loss of enzyme activity (Table 1). The initial screening was performed by incubating a fixed concentration of compounds **1**–**13** with cathepsin B under a pseudo-first order condition. A small aliquot of the incubation mixture was withdrawn at a fixed time interval and the remaining cathepsin B activity was measured in a large volume of assay mixture (17.5-fold dilution) containing cathepsin B substrate. The IC_{50} values were deliberately not estimated for this library, since they are not considered a good yardstick for measuring a time-dependent irreversible loss of enzyme activity due to a non-equilibrium binding mechanism.[31]

Compounds **1** and **2** which bear a non-polar 4-fluorophenyl and a propyl substituent respectively at the second carbon of the oxirane ring were non-inhibitory. This result indicated that a second substitution at the oxirane moiety in this class of molecules was perhaps detrimental to their inhibitory efficacies. Furthermore, compound **12**, which incorporates a methylene linker between the arylsulfonyl group and oxirane moiety, was also inert. We surmised that the lack of reactivity of **12** could presumably be due to lack of assistance from a general acid appropriately positioned in the cathepsin B active site to promote nucleophilic opening of oxirane ring by Cys29-S_γ residue. So, a thiirane analogue, **13**, that potentially contains a better leaving group thiolate (compared to alkoxide in **12**), was synthesized, and was also found to be ineffective. This again indicated that appropriate positioning of arylsulfonyl group with respect to the reactive oxirane group within the cysteine cathepsin active site was critically important for its inhibition. Efforts then became focused on synthesizing analogues of 2-(arylsulfonyl)oxiranes where functional variations of the aryl ring was further investigated.

Among the synthesized library, compound **5** was found to be most effective in inhibiting cysteine cathepsin B activity. The effectiveness of compound **5** was evident from a progressive loss of enzyme activity when it was incubated with active cathepsin B (Fig. 1A). No gain in cathepsin B activity was observed even after dilution of **5**–inactivated cathepsin B complex, thereby indicating that the mechanism of inhibition was perhaps covalent and irreversible in nature (data not shown). To assess the inhibitory efficacy, inactivation experiments were performed at appropriate concentrations of compound **5** under pseudo-first order conditions, and the experimental data thus obtained were analyzed using a simple two-step inhibition model (Fig. 1B):

$$E + I \overset{K_i}{\rightleftharpoons} E \cdot I \overset{k_i}{\rightarrow} E - I$$

where K_i represents the reversible equilibrium binding constant for the first step, and k_i is the first order inactivation rate constant for the second irreversible step. To obtain these two parameters, the following procedure was adopted. The pseudo-first order rate constants of inactivation (k_{obs}) were obtained at appropriate concentration of **5** ([I] ≫ [cathepsin B]), and a Kitz–Wilson analysis was performed to fit the experimentally obtained data (Fig. 1C).[32] This procedure yielded the equilibrium binding constant (K_i = 86 ± 3 μM) for the first equilibrium binding step, and the first order

Table 1
General chemical structure and time-dependent inhibitory screen of human liver cathepsin B by the synthesized sulfonyloxirane library compounds

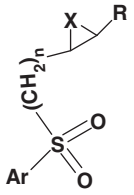

General Chemical Structure

Compound ID	Chemical structure (name)	% Inhibition
1	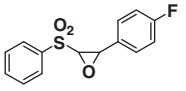 2-(4-fluorophenyl)-3-(phenylsulfonyl) oxirane	NI[a]
2	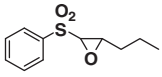 2-(phenylsulfonyl)-3-propyloxirane	NI[a]
3	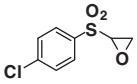 2-((4-chlorophenyl)sulfonyl)oxirane	44
4	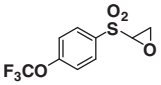 2-(4-(trifluoromethoxy)phenylsulfonyl)oxirane	30
5	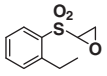 2-(2-ethylphenylsulfonyl)oxirane	>98
6	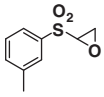 2-(m-tolylsulfonyl)oxirane	40
7	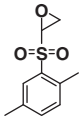 2-(2,5-dimethylphenylsulfonyl)oxirane	42
8	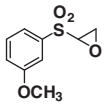 2-(3-methoxyphenylsulfonyl)oxirane	35
9	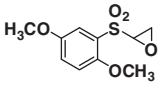 2-(2,5-dimethoxyphenylsulfonyl)oxirane	25

(*continued on next page*)

Table 1 (*continued*)

Compound ID	Chemical structure (name)	% Inhibition
10	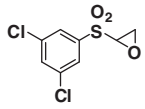 2-(3,5-dichlorophenylsulfonyl)oxirane	50
11	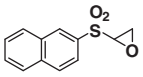 2-(naphthalen-3-ylsulfonyl)oxirane	18
12	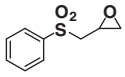 2-((phenylsulfonyl)methyl)oxirane	NI[a]
13	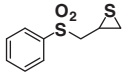 2-((phenylsulfonyl)methyl)thiirane	NI[a]

The initial screening for time-based inactivation was performed at 500 μM inhibitory concentrations under pseudo-first order condition ([I] ≫ [E]; cathepsin B = 175 nM). The enzyme activity was measured using a standard cathepsin B substrate after 10 min of incubation, as described in the enzyme assay protocol section.

[a] NI: No measurable time-dependent inhibition.

inactivation rate constant (k_i = 0.21 ± 0.01 min^{-1}) for the second irreversible step. We further investigated if the time-dependent inhibition of cathepsin B by **5** could be alleviated in the presence of a known active site-directed cathepsin B inhibitor, leupeptin (K_i = 5 nM).[33] This is mainly because if inhibitor **5** were to be an active-site directed agent, the rate of **5**-mediated cathepsin B inactivation reaction would be retarded in presence of a competitive inhibitor competing for the binding to the same active site.[34] A protection from inhibition of cathepsin B was indeed observed in presence of leupeptin, thereby indicating that **5** occupied the core cathepsin B active site that harbors the low pK_a nucleophilic Cys29 residue (Fig. 1D). A MALDI-based mass spectrometric analysis of the **5**–inhibited cathepsin B complex showed the expected mass increase of 212.1 amu in the cathepsin B protein. No further mass increase was observed even after prolonged incubation of **5** with cathepsin B. This result indicated that the mode of inhibition by **5** was indeed covalent and irreversible in nature and the stoichiometry of inhibition was likely 1:1 (Fig. 1E). This was important to establish since most cysteine cathepsins do contain multiple cysteines, in addition to the nucleophilic active site cysteine residue.[18]

2.2. Computational analysis of 5–inhibited cysteine cathepsin B complex

To understand the potential molecular interactions of **5** with cysteine cathepsin B in the covalently inhibited complex, computational modeling studies were performed. The CA073-inhibited complex of cathepsin B (PDB id: 2DC6) was appropriately modified to incorporate the inhibitor **5** covalently linked to Cys29-S_γ of cathepsin B active site. A molecular dynamic simulation (100 ps) was performed on the inhibitory complex and the trajectories of the molecular dynamics simulation were analyzed. Several interactions between the inhibitor **5** and cathepsin B active site were noteworthy (Fig. 2). While the O3 of sulfonyl oxygen formed a h-bond (3.4 Å) with the side chain of Gln23-N_ε—a key oxyanion hole residue, its O2 atom was engaged in a robust hydrogen bond interactions (2.8 Å) with a tightly-bound active site water molecule (Wtr12). The OH group of inhibitor was also stabilized with two h-bond interactions, one with the backbone carbonyl of a S2 site residue Gly198 (3.1 Å) and the other with an active site water (Wtr56) molecule (2.5 Å). The phenyl moiety of the inhibitor was found to be involved in a hydrophobic interaction with a non-polar patch containing Met196, Gly197, and Gly198 residues of S2 pocket. In addition, the *ortho*-ethyl group interacted with CH–π interactions with the aromatic side chains of Trp221 and His110 from S2′ pocket, albeit weakly.[35] A conclusive design of future inhibitory ligands that are selective towards individual members of the cysteine cathepsin family will require a structural elucidation of **5**-inhibited cysteine cathepsin complex using X-ray crystallography. Our modeling study suggests that *ortho*-substituted aryl groups containing a negatively charged group could prove to be selective inhibitory agents towards cathepsin B. Notably, cathepsin B is a unique member of cysteine cathepsins in that it exhibits endopeptidase, peptidyldipeptidase and carboxypeptidase activities.[36–38] This broad substrate specificity of cathepsin B has been ascribed to its unique structural feature that contains a flexible occluding loop (residues 104–126). Since His110 and His111 are part of this occluding loop, securing potential interactions from this loop could result in enhanced selectivity and potency towards cathepsin B. Such features could be exploited in designing selective inhibitors of cathepsin B.

2.3. Compound 5 is inert to external nucleophile and inhibits cysteine cathepsins selectively

To evaluate if the presence of an external nucleophile could compromise the inhibitory efficacy of **5**, we carried out cathepsin B inactivation kinetics in the presence of a strong nucleophile, azide ion (1 mM). No measurable change in inactivation kinetics was evident thereby indicating that compound **5** is relatively inert to an external nucleophile and unleashes its covalent reactivity only upon binding to the cathepsin B active site (data not shown).

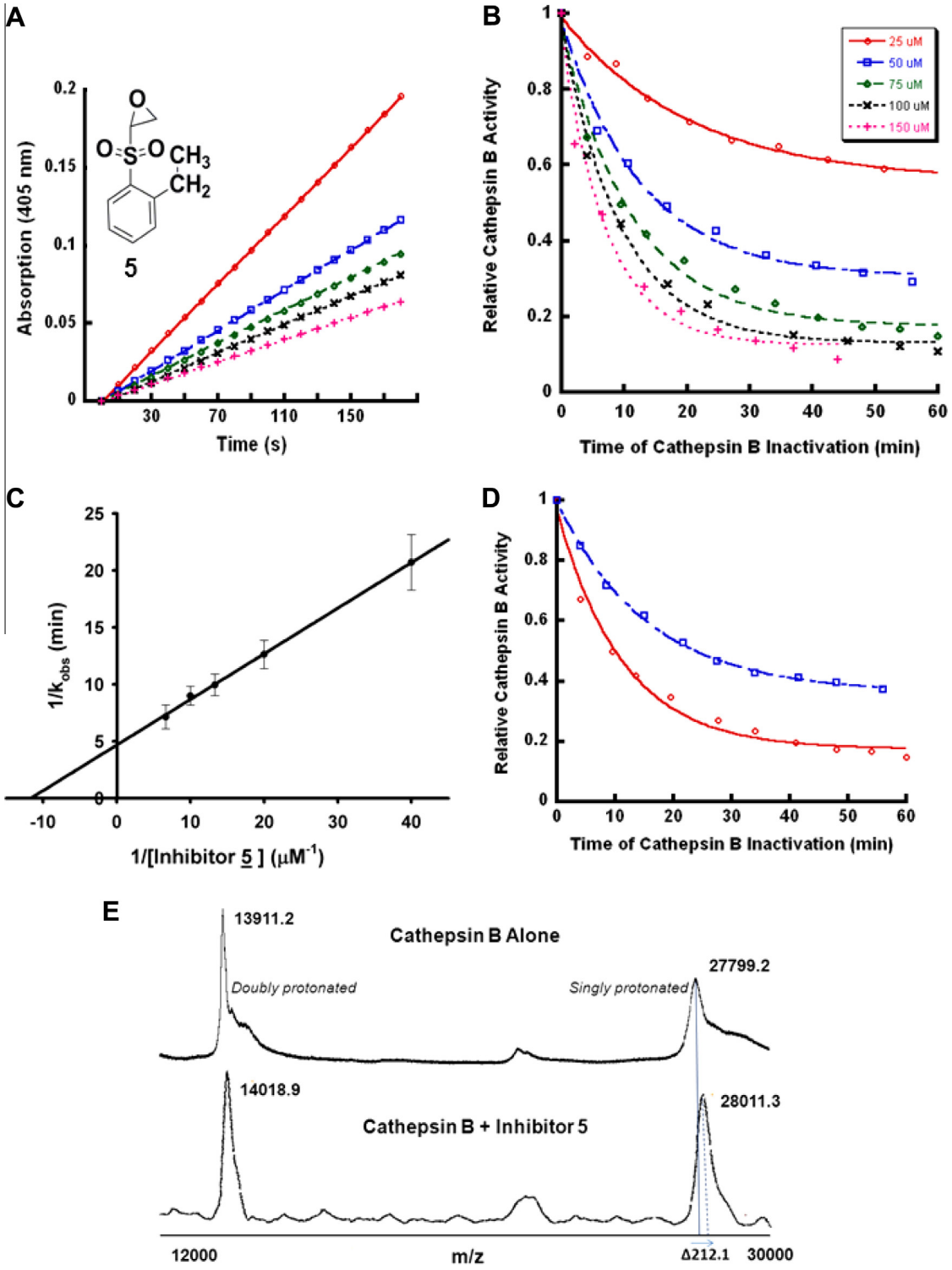

Figure 1. The mechanistic investigation of **5**-mediated cathepsin B inhibition. [A] Progress curves indicating a time-dependent loss of cathepsin B activity. Compound **5** was incubated with cathepsin B under pseudo-first order condition, and the progress curves were obtained at appropriate times of inactivation (red: 0 min, blue: 11 min, green: 17 min, black: 25 min, and pink: 41 min) using a chromogenic substrate Z-RR-*para*-nitroanilide. [B] Concentration-dependent loss of Cathepsin B activity with time. The points are experimental, and the lines joining them are fitted to obtain the pseudo-first order inactivation rate constants (k_{obs}). [C] Kitz–Wilson plot of **5**-mediated cathepsin B inactivation kinetics. The data points are fitted to a line that yields (a) $K_i = 86 \pm 3$ μM for the first equilibrium step of inhibitor binding, and (b) $k_i = 0.21 \pm 0.01$ min^{-1} for the first order inactivation rate constant for the second step. [D] The rate of **5**-mediated cathepsin B inhibition is decreased in the presence of leupeptin (40 nM; blue line), a known competitive inhibitor of cathepsin B, compared to the control (5% DMSO; red line). This experiment suggests that **5** is an active site-directed competitive inhibitor. [E] A mass spectrometric analysis of **5**–inhibited cathepsin B complex. A mass difference of 212.1 amu, consistent with the molecular weight of **5** (212.1), is observed in singly charged **5**–inhibited cathepsin B complex (lower panel) compared to uninhibited cathepsin B enzyme (upper panel). This experiment demonstrates that the mechanism of **5**-mediated cathepsin B inhibition is covalent and irreversible in nature.

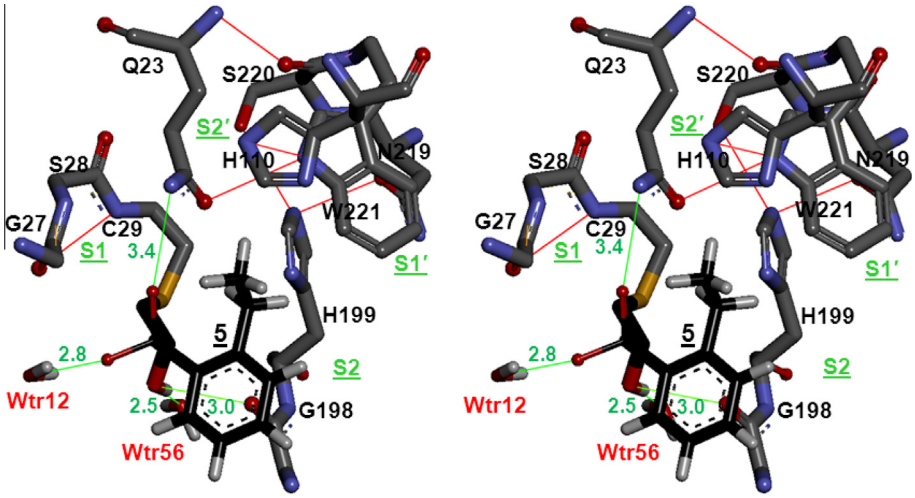

Figure 2. Stereoscopic view of the energy-minimized structure of covalently modified **5**–cathepsin B complex. The low pK_a active site Cys29 residue is the site for **5**-mediated covalent modification. For clarity, only the inhibitor **5** (black) and the key cathepsin B active site residues are shown. The key H-bonding distances of **5** with cathepsin B are shown in green. The intramolecular H-bonding interactions among cathepsin B active site residues near the inhibitor binding site are depicted in red (heavy atom h-bond donor and acceptor atoms cut off is 3.6 Å). The position of the primed and non-primed binding pockets on cathepsin B surface is shown in green text with underline.

The selectivity of inhibition of compound **5** towards cysteine cathepsins was investigated next. To do so, a panel of distinct family of enzymes were chosen and their inhibition by **5** was assessed (Table 2). While inhibition of cathepsin B by **5** was about 1.9-fold more selective compared to other two prominent members of cysteine cathepsins, namely cathepsin F and cathepsin S, an aspartyl-utilizing cathepsin D was only weakly (1/38th fold compared to cysteine cathepsin B) inhibited. Cathepsin G and trypsin protease that use a Ser nucleophile for catalysis remained inert to inhibition. These experiments suggested that compound **5** is selective towards cysteine cathepsins that utilize the uniformly conserved and reactive Cys residue for catalysis. The ability of compound **5** to inhibit protein tyrosine phosphatases (PTPs) was also evaluated. This enzyme utilizes a low pK_a Cys residue in nucleophilic catalysis. Although 2-(arylsulfonyl)-oxiranes were previously reported to be modest inhibitors of PTPs,[39] this enzyme also remained inert to inhibition by **5**. No apparent inhibition was observed with the prototypical PTP, hPTP1B, even at a concentration as high as 1 mM and after a prolonged incubation of one hour. While a conclusive analysis of this selectivity pattern towards cysteine cathepsins will require structural elucidation of the **5**–inhibited cathepsin B complex, it appears that the presence of an ethyl group at the *ortho* position of 2-(phenylsulfonyl)oxirane is significantly favored for binding at the cysteine cathepsin active site.

Table 2
Selectivity of inhibition of compound **5** towards cysteine cathepsins as assessed by the 2nd order enzyme inactivation rate constants

Enzyme (enzyme family)	2nd Order inactivation Rate constant (M^{-1} min^{-1})
Cathepsin B (cysteine cathepsin)	2441 ± 202[a]
Cathepsin F (cysteine cathepsin)	1300 ± 208[b]
Cathepsin S (cysteine cathepsin)	1196 ± 96[b]
Cathepsin D (aspartyl cathepsin)	65 ± 5[b]
Cathepsin G (serine cathepsin)	NI[c]
Trypsin (serine protease)	NI[c]
hPTP1B (protein tyrosine phosphatase)	NI[c]

[a] Calculated from the k_i and K_i parameters obtained using Kitz–Wilson analysis.
[b] Determined by measuring pseudo-first order rate constant of inactivation k_{obs} first and dividing the k_{obs} by the inhibitor concentration.
[c] NI: No apparent time-dependent inhibition even at a concentration as high as 1 mM during a 1-h inactivation reaction.

2.4. Compound 5 is cell permeable and inhibits intracellular cysteine cathepsin activity in metastatic human breast carcinoma MDA-MB-231 cells

Before proceeding to evaluate the cellular efficacy of **5** to inhibit cysteine cathepsins in human cells, it was important to establish its hydrolytic stability at physiological pH. This consideration was prompted by the oxirane functionality in **5** which could become hydrolytically unstable as a result of the adjacent electron-withdrawing sulfonyl moiety. This could render the inhibitor unsuitable for biological applications. Using NMR-based experiments, the half-life of **5** at physiological pH (pH 7.4) was found to be 3.6 h (Supplementary data, Fig. S1). This study suggested that compound **5** was relatively stable at physiological pH, and therefore could be used as an important tool in biological applications.

Cysteine cathepsins play important functional roles in both intracellular and extracellular signaling events.[40] Contrary to popular belief, recent studies strongly suggest that within the cell, active cysteine cathepsins play regulatory roles in distinct cellular compartments other than lysosomes, such as nucleus, mitochondrial matrix, cytoplasm, and plasma memebrane.[4,41,42] For example, a mis-regulated and an enhanced proteolytic activity of cytoplasmic cysteine cathepsins have shown to be linked to tumor invasion.[40] Indeed, the invasion potential of both human melanoma and prostate carcinoma cells was found to be significantly reduced only when these cells were subjected to cell membrane permeable cysteine cathepsin inhibitors, thereby suggesting the importance of intracellular cathepsins and their effective inhibition.[43] Similarly, a study by Sloane and co-workers in human breast carcinoma BT549 cells suggested that only cell-permeable cysteine cathepsin inhibitors were able to reduce the intracellular proteolysis in these cells.[44] These investigations together underscore the importance of developing non-peptidyl and cell permeable small molecule inhibitors of cysteine cathepsins, so that their precise function can be annotated in both normal physiology and human diseases. Unfortunately, cell-permeable and non-peptidyl inhibitory agents of cysteine cathepsins remain scarcely available today.

Thus in an initial approach, we assessed whether **5** had the potential to inhibit intracellular cysteine cathepsin B activity in living cells. The metastatic MDA-MB-231 human breast cell line was chosen for this study since it has been shown that cysteine cathepsin B

activity is upregulated in these cells.[45] A highly efficient and specific cathepsin B substrate, Z-RR-AMC ($k_{cat}/K_m = 10^5\ M^{-1}\ s^{-1}$), previously employed in cell-based experiments, was chosen for this study.[46,47] While efficient proteolysis of the substrate was evident in control MDA-MB-231 cells, a significant loss of intracellular cathepsin B activity was observed in **5**-treated cells (Fig. 3A). Furthermore, intracellular cathepsin B activity was shown to decrease in a dose-dependent manner (Fig. 3B).

In a second approach, the usefulness of **5** to inhibit cellular cysteine cathepsin activity in cells was also investigated using a physiologically relevant proteolytic protein target of cysteine cathepsin B and S, namely E-cadherin, an adherens junction protein.[12] The integrity of this epithelial adhesion protein is critically important in maintaining both intercellular contacts and cellular morphology.[48–50] While it has been shown that a mere loss of cell–cell contacts alone is not sufficient to promote metastasis, a loss of E-cadherin alone has been shown to be sufficient to induce this behavior through epithelial-to-mesenchymal transition (EMT), enhanced motility, resistance to apoptosis, and invasiveness.[51] The majority of human tumors are carcinomas that originate from cells of epithelial tissues where a complete or a partial loss of E-cadherin occurs as the tumor progressively becomes malignant.[52–54] Thus, the loss of E-cadherin has been directly linked to invasive migratory behavior of cancer cells.[51,55] In a study involving metastatic MDA-MB-231 breast cancer cells which expresses very low levels of E-cadherin,[54] the re-expression of E-cadherin led to the restoration of normal E-cadherins-mediated cell–cell junctions, and a reversion to a normal epithelial morphology.[56] We therefore evaluated the levels of E-cadherin in MDA-MB-231 cells using an E-cadherin antibody in the presence and absence of inhibitor **5**. As anticipated, a dose-dependent increase in the levels of E-cadherin was observed in a population of **5**-treated MDA-MB-231 cells, as compared to control cells treated only with DMSO (Fig. 4A and B). It should also be noted that the overall cellular morphology of metastatic MDA-MB-231 cells also changed upon inhibitory treatment (Figs. 3A and 4A). This perhaps is not too

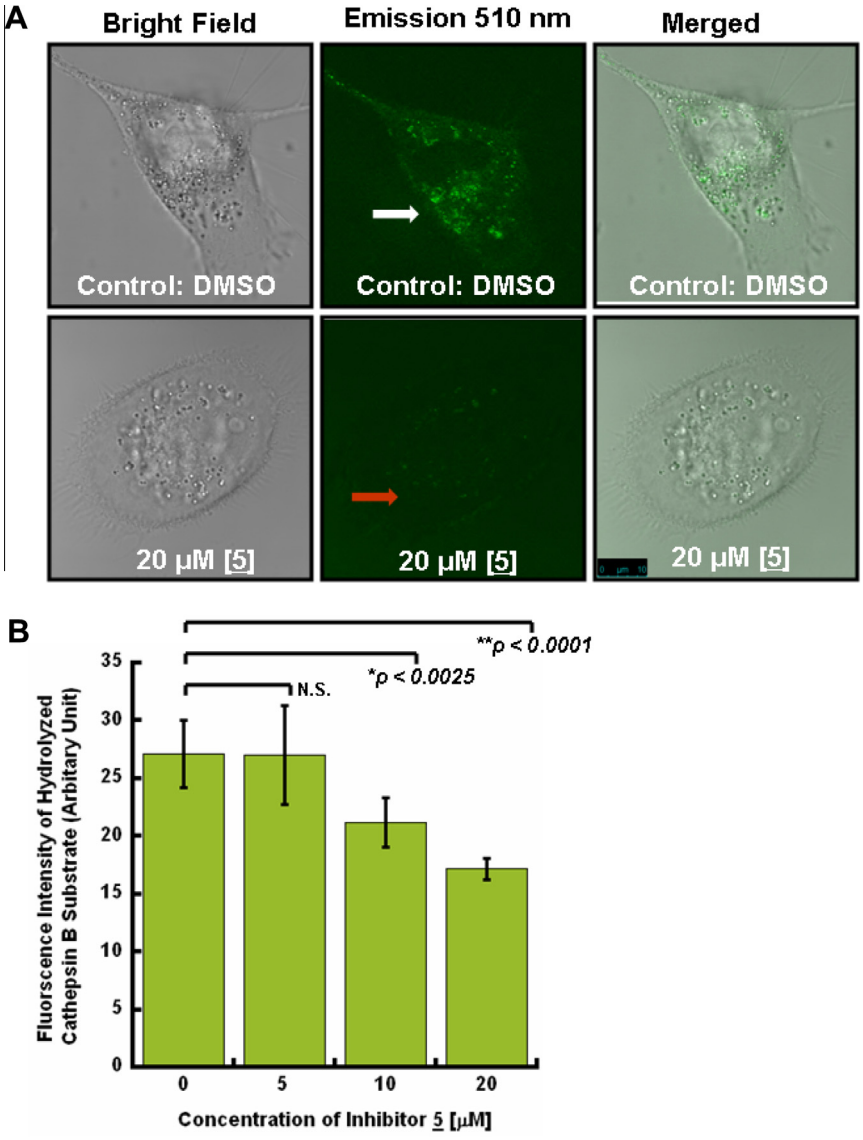

Figure 3. Effect of inhibitor **5** on cathepsin B activity in breast cancer MDA-MB-231 cells. [A] Cells were incubated with vehicle (DMSO 0.1%) and 20 μM of **5** for 20 min, followed by an additional 10 min of incubation with the substrate Z-RR-AMC (25 μM net) of **5**. Images show a significant loss of signal intensity (green) from the enzymatic turnover of the fluorophore cathepsin B substrate Z-RR-AMC (shown by red arrow in the bottom panel) at 20 μM of **5**. The control experiment without **5** indicates that a high level of substrate turnover occurs in these cells, thereby indicating a robust cathepsin B activity (white arrow—top panel). Scale bar = 10 μm. [B] The dose-dependent inhibition of intracellular cysteine cathepsin B activity with inhibitor **5** as measured by average fluorescence intensity over the entire cell. Note: The fluorescent intensity values are mean ± S.D. calculated over a population of at least 5–8 cells for each condition. *Statistical significance was evaluated by the Student's *t*-test.

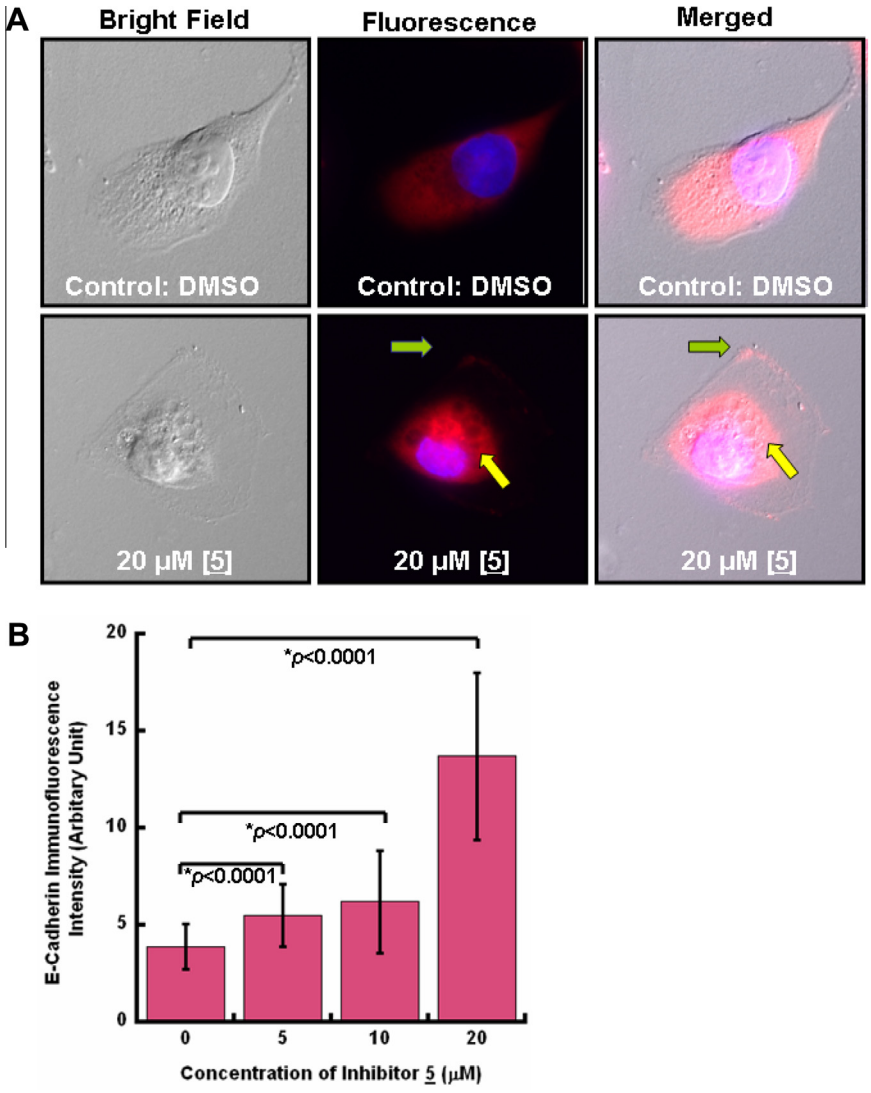

Figure 4. A physiological substrate of cysteine cathepsins, E-cadherin, is enriched in **5**-treated MDA-MB-231 breast cancer cells. [A] E-cadherin expression levels as detected by immunofluorescence in MDA-MB-231 cells. Cells were treated with control (0.1% DMSO) and cysteine cathepsin-B inhibitor **5** (20 μM) for 20 min, fixed, and then stained for E-cadherin. Bright field and merged fluorescence images of E-cadherin (red) and nuclear stain Hoechst 33342 (blue signal) are shown. Green and yellow arrows show enhanced E-cadherin levels (red) near the cell periphery (green arrow) and perinuclear region (yellow arrow) respectively in **5**-treated cell, compared to control (0.1% DMSO). Scale bar = 10 μm. [B] A dose-dependent increase of E-cadherin expression levels from immunocytochemistry as measured by average fluorescence intensity over the cell-periphery. The fluorescence intensity values are mean ± S.D. calculated over a population of 28 cells for each condition. *Statistical significance was evaluated by the Student's *t*-test.

surprising since cellular enrichment of E-cadherin is known to have a direct impact on cellular morphology.[48,49] Further experiments will be required to investigate the molecular basis of altered cellular morphology in MDA-MB-231 cells upon inhibitory treatment. A Western blot analysis of **5**-treated MDA-MB-231 cells was also performed that exhibited an enrichment of E-cadherin levels in **5**-treated cells, as compared to the control cells (see Supplementary data, Fig. S2). Collectively, these studies demonstrated that **5** was effective in inhibiting the intracellular activity of cysteine cathepsins in the invasive MDA-MB-231 breast cancer cells.

Finally to demonstrate that inhibition of cysteine cathepsins by **5** has a functional relevance in metastatic MDA-MB-231 breast cancer cells, a study involving cell migration behavior was planned. An enrichment of E-cadherin levels, as a result of inhibition of cysteine cathepsins by **5**, is anticipated to exhibit a reduced cell migratory behavior in a metastatic cancer cell line.[57,58] Thus, a cell motility assay was carried out in presence (10 and 20 μM) and absence (control, 0.05% DMSO) of inhibitor **5** using metastatic MDA-MB-231 cells. As anticipated, a dose-dependent decrease in cell migratory behavior of metastatic MDA-MB-231 cells was observed (Fig. 5). This experiment supported the notion that the compound **5** was effective in inhibiting the cell migratory potential of these highly metastatic cells.

3. Conclusions

We have developed a new class of small molecule inhibitors of cysteine cathepsins. A detailed kinetic and mass spectrometric analysis was performed to determine the kinetic parameters and mode of inhibition. The covalent inhibition of compound **5** was found to be selective towards cysteine cathepsins. The mechanistically distinct enzymes, such as aspartyl cathepsin D, serine cathepsin G, serine protease trypsin and a low pK_a cysteine-containing enzyme protein tyrosine phosphatase 1B, were not inhibited by **5**. Molecular modeling studies of the **5**–inhibited cysteine cathepsin B complex indicated that **5** interacted favorably with

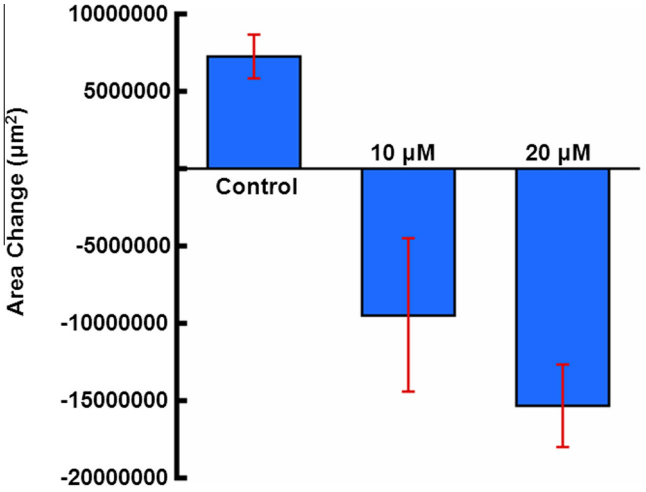

Figure 5. The effect of cysteine cathepsin inhibitor **5** on the cell-migratory behavior of metastatic human breast cancer MDA-MB-231 cells. The cell migration phenotype was reduced upon treatment of cells with compound **5** (10 and 20 µM), compared to control (0.05% DMSO). Each reported change in area value is the average of triplicate measurements with the corresponding standard deviation value.

the key active site residues surrounding S1 and S2 pockets. The inhibitor **5** was shown to be stable to spontaneous hydrolysis, cell-permeable, and effective in inhibiting intracellular cysteine cathepsin B activity in metastatic human breast carcinoma MDA-MB-231 cells. We also demonstrated that compound **5** was effective in reducing the migratory potential of the metastatic MDA-MB-231 breast cancer cell lines. This class of inhibitory agents has potential applications in the construction of selective activity-based cysteine cathepsin probe, and towards the development of specific inhibitory agents for the individual members of cysteine cathepsins.

4. Experimental section

4.1. Synthesis

4.1.1. General

^{13}C NMR and ^{1}H spectra were recorded on a Brucker DPX 400 MHz FT NMR with automatic sample changer. Chemical shifts (δ) are reported in parts per million (ppm) and referenced to residual solvent peaks in the deuterated solvent, $CDCl_3$ (7.26 ppm for ^{1}H and 77.0 ppm for ^{13}C), DMSO (2.50 ppm for ^{1}H and 39.5 ppm for ^{13}C), $(CD_3)_2CO$ (2.05 ppm for ^{1}H and 29.9, 206.7 for ^{13}C) and CD_3OD (4.87, 3.31 for ^{1}H and 49.1 for ^{13}C). Coupling constants (J) are reported in Hertz (Hz) and multiplicities are abbreviated as singlet (s), doublet (d), doublet of doublets (dd), triplet (t), triplet of doublets (td), and multiplet (m). The following materials were purchased from Matrix Scientific (Columbia, SC, USA) *m*-thiocresol, 3-methoxybenzenethiol, 3,5-dichlorothiophenol, 2,5-dimethylthiophenol, 4-(trifluoromethoxy)thiophenol, 2-ethylthiophenol and 2,5-dimethoxythiophenol. Thiophenol, 2-naphthalenethiol, chloromethyl phenyl sulfone, 4-fluorobenzaldehyde, butyraldehyde, disodium salt of silica gel (Merck, grade9385, 230–400 mesh, 60 Å) were purchased from Sigma–Aldrich (St. Louis, MO, USA). Sodium hydroxide, hydrochloric acid, sodium chloride, sodium sulfate, ammonium chloride, and solvents were purchased from Fisher Scientific Inc. (Pittsburgh, PA, USA).

4.1.2. 2-(4-Fluorophenyl)-3-(phenylsulfonyl)oxirane (1)

The synthesis of this compound was achieved in a single step by appropriate modification of a published protocol.[59] The procedure involved a 1-h long reaction of 4-fluorobenzaldehyde with (chloromethylsulfonyl)benzene at room temperature in the presence of a phase transfer catalyst, tetra-*n*-butylammonium bromide (10 mol %), in toluene and potassium hydroxide solution. The final purification was performed using silica gel-based flash chromatography procedure that yielded compound **1** as a white solid. R_f = 0.28 Hexane:EtOAc (9:1). Yield: 90%. ^{1}H NMR (400 MHz, $CDCl_3$) δ ppm: 4.16 (d, J = 1.4 Hz, 1H), 4.58 (d, J = 1.4 Hz, 1H), 7.06 (m, 2H), 7.24 (m, 2H), 7.64 (m, 2H), 7.75 (m, 1H), 7.99 (m, 2H). ^{13}C NMR (125 MHz, $CDCl_3$); δ ppm 56.94, 70.95, 116.11 (d, J_{C-F} = 22.3 Hz, 2C intensity), 128.00 (d, J_{C-F} = 8.5 Hz, 2C intensity), 128.53 (d, J_{C-F} = 3.3 Hz, 1C), 128.88 (2C intensity), 129.56 (2C intensity), 134.70, 136.77, 163.49 (d, J_{C-F} = 250 Hz, 1C intensity). LRMS [ESI-MS +ve] calculated for ($C_{14}H_{11}FO_3S$+Na): 301.03, observed: 301.25.

4.1.3. 2-(Phenylsulfonyl)-3-propyloxirane (2)

This compound was synthesized using the same synthetic protocol as outlined in the synthesis of **1**. The final purification was performed using silica gel-based flash chromatography procedure that yielded compound **2** as a viscous oil. R_f = 0.22 Hexane:EtOAc (9:1). Yield: 85%. ^{1}H NMR (500 MHz, $CDCl_3$) δ ppm: 0.94 (t, J = 7.4 Hz, 3H) 1.47 (m, 2H), 1.57 (m, 1H), 1.66 (m, 1H), 3.63 (m, 1H), 3.90 (d, J = 1.6 Hz, 1H), 7.58 (m, 2H), 7.68 (m, 1H), 7.91 (m, 2H). ^{13}C NMR (125 MHz, $CDCl_3$) δ ppm: 13.63, 18.93, 32.22, 57.79, 68.30, 128.69 (2C intensity), 129.41 (2C intensity), 134.43, 137.08. LRMS [ESI-MS +ve] calculated for ($C_{11}H_{14}O_3S$+Na): 249.06, observed: 249.25.

4.1.4. 2-(4-Chlorophenylsulfonyl)oxirane (3)

This compound was synthesized by following an earlier published protocol.[39] The final purification was performed using silica gel-based flash chromatography procedure that yielded compound **3** as a white powder. R_f = 0.50 (hexane/EtOAc = 9/1). Yield: 63%. ^{1}H NMR (400 MHz, $CDCl_3$) δ ppm: 3.07 (dd, J = 5.4 and 3.7 Hz, 1H), 3.37 (dd, J = 5.4 and 2.1 Hz, 1H), 4.05 (dd, J = 3.7 and 2.1 Hz, 1H), 7.52 (d, J = 8.6 Hz, 2H), 7.81 (d, J = 8.6 Hz, 2H). ^{13}C NMR (100 MHz, $CDCl_3$) δ ppm: 45.54, 63.25, 129.84 (2C intensity), 130.31 (2C intensity), 135.25, 141.55. LRMS [ESI-MS +ve] calculated for ($C_8H_7ClO_3S$+H): 218.99, observed: 219.00.

4.1.5. 2-((4-Trifluoromethoxy)phenylsulfonyl)oxirane (4)

This compound was synthesized by following a published protocol.[39] The final purification was performed using silica gel-based flash chromatography procedure that yielded compound **4** as white semi-solid. R_f = 0.29 (hexane/EtOAc = 19/1). Yield: 40%. ^{1}H NMR (400 MHz, $CDCl_3$) δ ppm: 3.16 (dd, J = 5.3 and 3.6 Hz, 1H), 3.46 (dd, J = 5.3 and 2.0 Hz, 1H), 4.14 (dd, J = 3.6 and 2.0 Hz, 1H), 7.43 (d, J = 8.8 Hz, 2H), 8.01 (d, J = 8.8 Hz, 2H). ^{13}C NMR (100 MHz, $CDCl_3$) δ ppm: 45.58, 63.24, 120.20 (q, J_{C-F} = 283 Hz), 121.10 (2C intensity), 131.22 (2C intensity), 134.99, 153.71. LRMS [ESI-MS +ve] calculated for ($C_9H_7F_3O_4S$+H): 269.01, observed: 269.00.

4.1.6. 2-(2-Ethylphenylsulfonyl)oxirane (5)

This compound was synthesized by following a published protocol.[39] The final purification was performed using silica gel-based flash chromatography procedure that yielded compound **5** as a pale yellow viscous oil. R_f = 0.28 (hexane/EtOAc = 19/1). Yield: 72%. ^{1}H NMR (400 MHz, $CDCl_3$) δ ppm: 1.32 (t, J = 7.4 Hz, 3H), 3.09 (q, J = 7.4 Hz, 2H), 3.11 (dd, J = 5.4 and 3.7 Hz, 1H), 3.40 (dd, J = 5.4 and 2.1 Hz, 1H), 4.19 (dd, J = 3.7 and 2.1 Hz, 1H), 7.42 (m, 2H), 7.61 (td, J = 7.7 and 1.2 Hz, 1H), 7.99 (dd, J = 8.0 and 1.2 Hz, 1H). ^{13}C NMR (100 MHz, $CDCl_3$) δ ppm: 16.15, 26.59, 44.87, 63.65, 126.64, 130.81, 131.33, 134.57, 134.92, 145.86. LRMS [ESI-MS +ve] calculated for ($C_{10}H_{12}O_3S$+H): 213.06, observed: 213.08.

4.1.7. 2-(*m*-Tolylsulfonyl)oxirane (6)

This compound was synthesized by following a published protocol.[39] The final purification was performed using silica gel-based flash chromatography procedure that yielded compound **6** as a colorless viscous oil. R_f = 0.39 (hexane/EtOAc = 9/1). Yield: 70%. ^{1}H NMR (400 MHz, $CDCl_3$) δ ppm: 2.46 (s, 3H), 3.12 (dd, *J* = 5.4 and 3.7 Hz, 1H), 3.41 (dd, *J* = 5.4 and 2.0 Hz, 1H), 4.13 (dd, *J* = 3.7 and 2.0 Hz, 1H), 7.49 (m, 2H), 7.75 (s, 2H). ^{13}C NMR (100 MHz, $CDCl_3$) δ ppm: 21.34, 45.35, 63.25, 125.92, 129.06, 129.33, 135.39, 136.66, 139.82. LRMS [ESI-MS +ve] calculated for ($C_9H_{10}O_3S$+H): 199.05, observed: 199.25.

4.1.8. 2-(2,5-Dimethylphenylsulfonyl)oxirane (7)

This compound was synthesized by following an earlier published protocol.[39] The purification using silica gel column chromatography yielded **7** as colorless viscous oil. R_f = 0.32 (hexane/EtOAc = 9/1). Yield: 68%. ^{1}H NMR (400 MHz, $CDCl_3$) δ ppm: 2. 39 (s, 3H), 2.67 (s, 3H), 3.10 (dd *J* = 5.3 and 3.7 Hz, 1H), 3.88 (dd, *J* = 5.3 and 2.1 Hz, 1H), 4.18 (dd, *J* = 3.7 and 2.1 Hz, 1H), 7.25 (d, *J* = 7.5 Hz, 1H), 7.35 (d, *J* = 7.5 Hz, 1H), 7.79 (s, 1H). ^{13}C NMR (100 MHz, $CDCl_3$) δ ppm: 20.33, 20.80, 44.68, 63.36, 131.03, 132.83, 134.87, 135.22, 136.31, 136.78. LRMS [ESI-MS +ve] calculated for ($C_{10}H_{12}O_3S$+H): 213.06, observed: 213.08.

4.1.9. 2-(3-Methoxyphenylsulfonyl)oxirane (8)

This compound was synthesized by following a published protocol.[39] The purification using silica gel column chromatography yielded **8** as a brownish viscous oil. R_f = 0.27 (hexane/EtOAc = 9/1). Yield: 70%. ^{1}H NMR (400 MHz, $CDCl_3$) δ ppm: 3.13 (dd, *J* = 5.4 and 3.7 Hz, 1H), 3.42 (dd, *J* = 5.4 and 2.0 Hz, 1H), 3.89 (s, 3H), 4.13 (dd, *J* = 3.7 and 2.0 Hz, 1H), 7.23 (ddd, *J* = 7.6, 2.5, and 1.9 Hz, 1H), 7.42 (dd, *J* = 1.9 and 1.6 Hz, 1H), 7.52 (m, 2H). ^{13}C NMR (100 MHz, $CDCl_3$) δ ppm: 45.31, 55.78, 63.25, 112.93, 120.94, 121.27, 130.54, 137.94, 160.15. LRMS [ESI-MS +ve] calculated for ($C_9H_{10}O_4S$+H): 215.04, observed: 214.83.

4.1.10. 2-(2,5-Dimethoxyphenylsulfonyl)oxirane (9)

This compound was synthesized by following a published protocol.[39] The purification using silica gel column chromatography yielded **9** as a white semi-solid. R_f = 0.24 Hexane:EtOAc (9:1). Yield: 78%. ^{1}H NMR (500 MHz, $(CD_3)_2CO$) δ ppm: 3.19 (dd, *J* = 5.6 and 3.7 Hz, 1H), 3.31 (dd, *J* = 5.6 and 2.0 Hz, 1H), 3.83 (s, 3H), 3.97 (s, 3H), 4.75 (q, *J* = 3.7 and 2.0 Hz, 1H), 7.28 (m, 3H).^{13}C NMR (125 MHz, $(CD_3)_2CO$) δ ppm: 44.56, 55.46, 56.47, 62.31, 114.07, 114.71, 121.83, 126.84, 151.82, 153.37. LRMS [ESI-MS +ve] calculated for ($C_{10}H_{12}O_5S$+H): 245.05, observed: 245.08.

4.1.11. 2-(3,5-Dichlorophenylsulfonyl)oxirane (10)

This compound was synthesized by following a published protocol.[39] The purification using silica gel column chromatography yielded **10** as a white powder. R_f = 0.67 (hexane/EtOAc = 9/1). Yield: 45%. ^{1}H NMR (400 MHz, $CDCl_3$) δ ppm: 3.18 (dd, *J* = 5.4 and 3.7 Hz, 1H), 3.48 (dd, *J* = 5.4 and 2.0 Hz, 1H), 4.16 (dd, *J* = 3.7 and 2.0 Hz, 1H), 7.69 (t, *J* = 1.8 Hz, 1H), 7.82 (d, *J* = 1.8 Hz, 2H).^{13}C NMR (100 MHz, $CDCl_3$) δ ppm: 45.54, 63.19, 127.18 (2C intensity), 134.61, 136.54 (2C intensity), 139.72. LRMS [ESI-MS +ve] calculated for ($C_8H_6Cl_2O_3S$+Na): 274.93, observed: 275.00.

4.1.12. 2-(Naphthalen-3-ylsulfonyl)oxirane (11)

This compound was synthesized by following a published protocol.[39] The purification using silica gel column chromatography yielded **11** as a white powder. R_f = 0.27 (hexane/EtOAc = 19/1). Yield: 78%. ^{1}H NMR (400 MHz, $CDCl_3$) δ ppm: 3.15 (dd, *J* = 5.4 and 3.7 Hz, 1H), 3.47 (dd, *J* = 5.4 and 2.1 Hz, 1H), 4.19 (dd, *J* = 3.7 and 2.1 Hz, 1H), 7.66 (m, 1H), 7.72 (m, 1H), 7.91 (dd, *J* = 8.6 and 1.8 Hz, 1H), 7.96 (d, *J* = 8.6 Hz, 1H), 8.03 (dd, *J* = 8.4 and 1.0 Hz, 1H), 8.06 (d, *J* = 8.4 Hz, 1H), 8.53 (d, *J* = 1.0 Hz, 1H).^{13}C NMR (100 MHz, $CDCl_3$) δ ppm: 45.43, 63.39, 123.09, 127.85, 128.06, 129.60, 129.71, 129.76, 131.02, 132.20, 133.69, 135.75. LRMS [ESI-MS +ve] calculated for ($C_{12}H_{10}O_3S$+H): 235.05, observed: 235.08.

4.1.13. 2-((Phenylsulfonyl)methyl)oxirane (12)

This compound was synthesized by following the literature-reported protocol[60] and its characterization was found to be consistent with the previously reported NMR spectra.[61]

4.1.14. 2-((Phenylsulfonyl)methyl)thiirane (13)

This compound was synthesized by following the literature-reported protocol[60] and its characterization was found to be consistent with the previously reported NMR spectra.[62]

4.2. Enzymology, physiochemical, and mass spectrometric studies

4.2.1. General

Following enzymes and their substrates were purchased from Enzo Life Sciences (Farmingdale, NY, USA): cathepsin B (BML-SE198), cathepsin D (BML-SE199), cathepsin S (BML-SE453), cathepsin F (BML-SE568), cathepsin G (BML-SE283), human PTP1B (BML-SE332), Z-Arg-Arg-pNA (BML-P138), Z-Arg-Arg-AMC (BML-P137), Z-Phe-Arg-AMC (BML-P139), Suc-Ala-Ala-Pro-Phe-pNA (BML-P141), Mca-Gly-Lys-Pro-Ile-Leu-Phe-Phe-Arg-Leu-Lys(Dnp)-D-Arg-NH_2 (BML-P145), Z-Val-Val-Arg-AMC (BML-P199). *N*-alpha-Benzoyl-DL-arginine-*p*-nitroanilide (BAPNA) (B4875), trypsin (T1426), leupeptin, *para*-nitrophenylphosphate and bovine serum albumin (A2153) were purchased from Sigma–Aldrich (St. Louis, MO, USA). All the biological grade buffers were used and were purchased from Sigma–Aldrich (St. Louis, MO, USA). All enzyme kinetics experiments (unless otherwise stated) were carried out at 30 °C in appropriate buffer condition with 5% DMSO concentration. The mass spectra were acquired using a MALDI-microMX mass spectrometer (Waters Corp., Milford, MA) instrument equipped with an N_2 laser operating at 10 Hz, using delayed extraction and positive ion linear mode analysis. For measuring the initial rates of enzyme catalyzed reaction, a temperature-controlled steady-state arc lamp fluorometer equipped with Felix 32 software (Photon Technology Instrument, Birmingham, NJ, USA) and a UV–Vis spectrophotometer (Model λ25; Perkin Elmer Inc., Waltham, MA, USA) was used.

4.2.2. Methodologies for assessing time-dependent inactivation of cysteine cathepsin B and inhibitor screening procedure

The inactivation reaction of human liver cathepsin B (net 175 nM) with inhibitor was performed under pseudo first order condition ([I] ≫ [E]) in a 0.5 ml eppendorf tube maintained at 30 °C in a temperature controlled bath. Freshly made inhibitor stock solution (in DMSO) was used for each experiment. A previously reported cathepsin B assay procedure was employed.[63,64] Cathepsin B enzyme was first activated for 10 min in sodium phosphate buffer (100 mM, pH 6.0) containing 5 mM DTT and 1 mM Na_2EDTA. The inactivation reaction was initiated by the addition of inhibitor where DMSO concentration was maintained at 5%. After suitable time intervals, an aliquot of 10 μl of incubation mixture was withdrawn and added to an assay mixture (net assay volume 175 μl) that contained 3 mM of Z-RR-pNA (K_m = 0.9 mM) substrate at 30 °C. A progress curve was recorded at 405 nM, and the enzyme activity was determined by measuring the initial rates of substrate turnover. For initial screening experiments, the assay protocol remained the same except that the concentration of all inhibitors was fixed at 500 μM and the residual enzyme activity was measured after 10 min of reaction.

4.2.3. Method for estimation of kinetic parameters for 5-mediated cathepsin B inhibition

To obtain K_i and k_i parameters for the two step inhibition model, the following procedure was adopted. A sequence of independent cathepsin B inactivation experiments were performed at 25, 50, 75, 100, and 150 μM of **5** under pseudo-first order condition ([I] ≫ [Cathepsin B]) and enzyme activities were monitored at appropriate time intervals. The data thus obtained at each concentration were plotted and fitted to the following equation $A_t = A_f - (A_f - A_0)e^{(-k_{obs} \times t)}$ where A_t = enzyme activity at time t of cathepsin B inactivation, A_f = final cathepsin B activity at infinite time of inactivation, A_0 = initial enzyme activity at zero time of inactivation, and k_{obs} = pseudo-first order rate constant of inactivation. Kitz–Wilson analysis is then performed to estimate the reversible equilibrium binding constant K_i for the first step, and the first order inactivation rate constant (k_i) for the second irreversible step, as described elsewhere.[32] For, demonstration that compound **5** is active site-directed, the inactivation reaction of **5** with cathepsin B was performed in presence of an established competitive inhibitor of cathepsin B, leupeptin (40 nM) and the residual cathepsin B activity was measured, as described above. Such a methodology has been previously utilized to demonstrate the active site-directed nature of inhibition for previously uncharacterized covalent and irreversible inhibitory agents.[34,65]

4.2.4. Cathepsin F inhibition assay

A previously reported enzyme assay procedure was adopted with appropriate modifications.[66] The enzyme was activated for 10 min in 50 mM potassium phosphate buffer at pH 6.5 containing 2.5 mM DTT, 2.5 mM Na_2EDTA, and 1.0 mg/ml BSA at 25 °C. The inactivation reaction was initiated by addition of inhibitor **5** to activated human cathepsin F (net 10.8 nM). After suitable time intervals, an aliquot of 10 μl of incubation mixture was withdrawn and the enzyme activity was measured in an assay buffer (net 175 μl) containing 3 μM of Z-FR-AMC fluorogenic substrate (K_m = 0.44 μM) at 25 °C.

4.2.5. Cathepsin S inhibition assay

For assaying cathepsin S activity, *a* previously published protocol was followed with appropriate modification.[67] Thus, cathepsin S enzyme was activated first in the 100 mM potassium phosphate buffer (pH 6.5) containing 5 mM DTT, 5 mM Na_2EDTA for 10 min. The inactivation reaction of human cathepsin S (net 134.6 nM) with inhibitor **5** (75 μM) was initiated. After suitable time intervals, an aliquot of 3 μl of incubation mixture was withdrawn and the enzyme activity was measured in assay buffer (175 μl; 8% DMSO) containing 250 μM of Z-VVR-AMC (K_m >100 μM;[68] Ex/Em: 365/440 nm) fluorogenic substrate.

4.2.6. Cathepsin G inhibition assay

A previously reported assay conditions were followed.[69] The enzyme was activated in 20 mM Tris–HCl buffer (pH 7.4) containing 500 mM NaCl for 15 min. The inactivation reaction of human cathepsin G (net 7.66 nM) with inhibitor **5** was initiated. After suitable time intervals, an aliquot of 10 μl of incubation mixture was withdrawn and the enzyme activity was measured in assay buffer containing 3.4 mM Suc-AAPF-pNA cathepsin G substrate (K_m = 1.7 mM).

4.2.7. Cathepsin D inhibition assay

The enzyme was activated in 50 mM sodium acetate buffer (pH 4) containing 5 mM DTT and 1 mg/ml bovine serum albumin. The inactivation reaction of human Cathepsin D (net 20 nM) with inhibitor was initiated. After suitable time intervals, an aliquot of 1 μl of incubation mixture was withdrawn and added to an assay mixture (net assay volume of 175 μl) that contained 40 μM of Mca-Gly-Lys-Pro-Ile-Leu-Phe-Phe-Arg-Leu-Lys(Dnp)-D-Arg-NH_2 [Mca = (7-methoxycoumarin-4-yl)acetyl] cathepsin D substrate (K_m = 3.7 μM). Enzyme activity was monitored by measuring fluorescent enhancement over the time.

4.2.8. Serine protease (trypsin) inhibition assay

The assay procedure was adopted from an earlier published protocol.[70] Trypsin enzyme solution was freshly made using 1 mM HCl just before the inactivation reaction. Inactivation reaction was initiated by the addition of inhibitor to a pre-activated trypsin (net concentration of 190–200 U/μl). After suitable time intervals, an aliquot of 2 μl incubation mixture were withdrawn and added to a 67 mM sodium phosphate assay buffer (net assay volume of 175 μl) which contained 3 mM *N*-alpha-benzoyl-DL-arginine-*p*-nitroanilide (BAPNA, K_m = 0.94 mM) as a substrate. Enzyme activity was monitored by measuring the initial rate of substrate consumption at 410 nm.

4.2.9. Protein tyrosine phosphatase 1B (PTP1B) inhibition assay

The time-dependent inactivation kinetics of **5** with PTP1B was performed as described before.[39]

4.2.10. Mass-spectral studies

Cathepsin B was activated and incubated with inhibitor **5** (800 μM) for 10 min under the conditions similar to those used for kinetics studies. Both **5**–inhibited cathepsin B inhibitory complex and control (5% DMSO) were prepared for matrix-assisted laser desorption/ionization mass spectrometry using the ultra-thin layer essentially as published.[71,72] Samples were saturated in a 1:9 ratio with a saturated solution of recrystallized α-cyano-4-hydroxycinnamic acid in 50% formic acid/33% isopropyl alcohol/17% water (v/v/v; Fisher Scientific-all HPLC grade). Acceleration potential of 12,000 V and an extraction pulse of 1950 V with a delay time for 410 ns were used. Spectra were smoothed and baseline corrected using MassLynx (Waters Corp.) and calibrated pseudo-internally using equine apomyoglobin.

4.2.11. Hydrolytic stability of inhibitor 5

To study the hydrolytic stability of compound **5**, NMR experiment was carried out in following manner. First, sodium phosphate buffer (10 mM) of pH 7.4 was prepared. A portion (5 ml) of this buffer was lyophilized and re-dissolved in deuterium oxide. This step was repeated thrice so as to ensure a complete H/D exchange. The buffer components were re-dissolved in deuterium oxide (5 ml). The hydrolysis experiment was carried out under pseudo first order reaction condition. A stock solution of **5**, freshly made in deuterated DMSO was added to deuterated phosphate buffer (total volume 500 μl; net concentration of **5** at 2.5 mM) and NMR spectra were recorded after appropriate time intervals (see Supplementary data, Fig. S1). The rate of hydrolysis was measured by comparing the integration values of initial and final compounds. The rate constant of hydrolysis was obtained by fitting the data to a single exponential decay curve ($I_t = I_0e^{-k \times t}$) and the half was calculated using the following equation: $t_{1/2} = 0.693/k$.

4.3. Molecular modeling

The molecular modeling studies were performed on a Dell PowerEdge 6000 server operating on Red Hat Enterprise Linux ES release 4. The $CH_3CONHCysCONHCH_3$ peptide covalently attached to inhibitor **5** at the terminal aliphatic carbon was built with open oxirane ring in Builder module of Maestro 7.5 software and partial charges on each atoms were determined in Jaguar (Schrodinger Inc., New York, NY, USA) using density-functional theory (DFT) calculation with B3LYP/6-31G* basis set. The coordinate file of cathepsin B (PDB id: 2DC6) was downloaded and appropriately

modified at pH 7.0 to include inhibitor **5** covalently linked to Cys29Sγ residue using Insight II software (Accelrys Inc., SanDiego CA, USA). The partial charges on the atoms of inhibitor were assigned from DFT calculations and the complex was soaked with a 15 Å spherical shell of water with Cys29Sγ as the center. The resulting complex was energy minimized (10,000 steps of Steepest Descent). A molecular dynamics run (100 ps) was then carried out on the energy-minimized complex using Consistent Valence Forcefield (CVFF) force field in Discover standalone program (Accelrys Inc., San Diego CA, USA). The trajectories from molecular dynamic run were saved every 2 ps and analyzed. During the energy minimation procedure and the molecular dynamics simulations, no constratins were imposed on **5**–cathepsin B inhibitor complex.

4.4. Biology

4.4.1. Cell culture

All the cell culture reagents were purchased from Invitrogen (Carlsbad, CA). MDA-MB-231 cells (American Type Culture Collection, Manassas, VA) were cultured on 10-cm plates (BD Falcon™) at 37 °C and 5% CO_2 in Iscove's Modified Dulbecco's medium with L-glutamine (IMDM), 10% fetal bovine serum, and antibiotics (1% penicillin/streptomycin and 0.5 μg/ml fungizone) as described earlier.[73] Cells were passaged at 1:3 ratio every 3–4 days and subcultured by 0.25% trypsin–EDTA treatment. Cells were re-plated one day prior to experiment so that the cell density was 70–80% on the day of the experiment.

4.4.2. Confocal microscopy

For live-cell imaging, cells were seeded to poly-D-lysine coated 35 mm-glass bottom dishes (MatTek; Ashland, MA) and grown overnight in complete medium. Prior to imaging, cells were treated in 15 mM HEPES containing phenol-red (PR)-free complete medium. To reduce photo-bleaching, 0.6u of Oxyrase enzyme per ml (Oxyrase Inc.) was added to the PR-free medium containing 10 mM sodium-lactate, as previously described.[74] Cells were incubated with either dimethylsufoxide (DMSO, 0.1% v/v) as vehicle control, or varying concentrations of **5** for 20 min at 37 °C, followed by an additional 10 min of incubation with the substrate Z-RR-AMC (25 μM net) of **5**. Images of cells were acquired using an inverted Leica TCS-SP5 confocal microscope (Leica; IL) by Plan apochromat 63 × 1.4 oil objective lens (numerical aperture 0.6–1.4). An argon ion laser (25%) was used to generate an excitation at 488 nm, and pinholes were typically set to 1–1.5 Airy units. Results for every condition are the average over three independent experiments in each of which 8–10 cells were analyzed by ImageJ.

4.4.3. Immunofluorescence

Cells, grown on 35-mm glass coverslips in 6-well plate for 24 h, were treated with the vehicle (0.1% DMSO), or appropriate concentrations of cathepsin B inhibitor for 20 min at 37 °C. After treatment they were fixed in 3.7% PFA at room temperature for 10 min followed by 30 s incubation in microtubule-stabilizing and cell-permeabilizing buffer (80 mM PIPES, 1 mM $MgCl_2$, 4 mM EGTA, 0.5% Triton-X100) at room temperature. The samples were then washed thrice with phosphate-buffered saline (PBS) and incubated in immunoblocker (2% BSA, 0.1% sodium azide) for 15 min at 37 °C.

For immunostaining, cells were incubated overnight at 4 °C with monoclonal mouse antibody E-cadherin (1:100) (Santa Cruz Biotechnology, Santa Cruz, CA) followed by incubation with secondary Alexa 594-conjugated donkey anti-mouse antibody (1:300) (Invitrogen, Carlsbad, CA) for 2 h at 37 °C.[49,75] DNA was stained with Hoechst 33342 (1 mg/ml in PBS). Cells were mounted on clean glass slides using mounting media DABCO (Invitrogen). Samples were examined with a Plan-Neofluar 40 × 0.75 oil immersion objective lens using a Zeiss Axio Imager-M2 upright fluorescence microscope (Zeiss, Heidelberg, Germany). Results for every condition are the average of three independent experiments in each of which 28 cells were analyzed by ImageJ software.

4.4.4. Cell motility assay

The effect of inhibitor **5** on cell migratory behavior of MDA-MB-231 cells was evaluated by following a slight modification of an earlier published protocol.[76] Thus MDA-MB-231 cells were plated as concentric circles on a 10-well glass slide pre-coated with 1% BSA through a 10-hole cell sedimentation manifold (CSM, Inc., Phoenix, AZ) followed by incubation at 37 °C and 5% CO_2. After removal of the manifold, cells were treated with control vehicle (0.05% DMSO) or appropriate concentrations of inhibitor **5**, and incubated for 6 h at 37 °C. Images were acquired by a digital camera (Moticam 2000) attached to an inverted Nikon Diaphot microscope both before (t0) and after inhibitory treatment (t6). Motility of cells was calculated by the change in total area (in square micrometers) by Image J software. Each reported value is the average of triplicate measurements with corresponding standard deviation value (S.D.).

Acknowledgments

The authors wish to gratefully acknowledge the funding support provided by the PSC-CUNY Research Award Program, and Queensborough Community College (QCC)/Queens College NSF-STEP and NIH Bridges programs.

Supplementary data

Supplementary data associated with this article can be found, in the online version, at http://dx.doi.org/10.1016/j.bmc.2013.03.062.

References and notes

1. Puente, X. S.; Gutierrez-Fernandez, A.; Ordonez, G. R.; Hillier, L. W.; Lopez-Otin, C. *Genomics* **2005**, *86*, 638.
2. Rawlings, N. D.; Barrett, A. J.; Bateman, A. *Nucleic Acids Res.* **2012**, *40*, D343.
3. Chwieralski, C. E.; Welte, T.; Buhling, F. *Apoptosis* **2006**, *11*, 143.
4. Reiser, J.; Adair, B.; Reinheckel, T. *J. Clin. Investig.* **2010**, *120*, 3421.
5. Joyce, J. A.; Hanahan, D. *Cell Cycle* **2004**, *3*, 1516.
6. Yasuda, Y.; Kaleta, J.; Bromme, D. *Adv. Drug Deliv. Rev.* **2005**, *57*, 973.
7. Maehr, R.; Mintern, J. D.; Herman, A. E.; Lennon-Dumenil, A. M.; Mathis, D.; Benoist, C.; Ploegh, H. L. *J. Clin. Investig.* **2005**, *115*, 2934.
8. Huang, X.; Vaag, A.; Carlsson, E.; Hansson, M.; Ahren, B.; Groop, L. *Diabetes* **2003**, *52*, 2411.
9. Rieux, A.; Gras, S.; Lecaille, F.; Niepceron, A.; Katrib, M.; Smith, N. C.; Lalmanach, G.; Brossier, F. *PLoS ONE* **2012**, *7*, e31914.
10. Vasiljeva, O.; Reinheckel, T.; Peters, C.; Turk, D.; Turk, V.; Turk, B. *Curr. Pharm. Des.* **2007**, *13*, 387.
11. Jedeszko, C.; Sloane, B. F. *Biol. Chem.* **2004**, *385*, 1017.
12. Gocheva, V.; Zeng, W.; Ke, D.; Klimstra, D.; Reinheckel, T.; Peters, C.; Hanahan, D.; Joyce, J. A. *Genes Dev.* **2006**, *20*, 543.
13. Vasiljeva, O.; Papazoglou, A.; Kruger, A.; Brodoefel, H.; Korovin, M.; Deussing, J.; Augustin, N.; Nielsen, B. S.; Almholt, K.; Bogyo, M.; Peters, C.; Reinheckel, T. *Cancer Res.* **2006**, *66*, 5242.
14. Sevenich, L.; Werner, F.; Gajda, M.; Schurigt, U.; Sieber, C.; Muller, S.; Follo, M.; Peters, C.; Reinheckel, T. *Oncogene* **2011**, *30*, 54.
15. Emmert-Buck, M. R.; Roth, M. J.; Zhuang, Z.; Campo, E.; Rozhin, J.; Sloane, B. F.; Liotta, L. A.; Stetler-Stevenson, W. G. *Am. J. Pathol.* **1994**, *145*, 1285.
16. Gocheva, V.; Joyce, J. A. *Cell Cycle* **2007**, *6*, 60.
17. Perl, A. K.; Wilgenbus, P.; Dahl, U.; Semb, H.; Christofori, G. *Nature* **1998**, *392*, 190.
18. Turk, V.; Stoka, V.; Vasiljeva, O.; Renko, M.; Sun, T.; Turk, B.; Turk, D. *Biochim. Biophys. Acta* **2012**, *1824*, 68.
19. Cravatt, B. F.; Wright, A. T.; Kozarich, J. W. *Annu. Rev. Biochem.* **2008**, *77*, 383.
20. Hanada, K.; Tamai, M.; Yamagishi, M.; Ohmura, S.; Sawada, J.; Tanaka, I. *Agric. Biol. Chem.* **1978**, *42*, 523.
21. Turk, D.; Podobnik, M.; Popovic, T.; Katunuma, N.; Bode, W.; Huber, R.; Turk, V. *Biochemistry* **1995**, *34*, 4791.
22. Yamamoto, A.; Hara, T.; Tomoo, K.; Ishida, T.; Fujii, T.; Hata, Y.; Murata, M.; Kitamura, K. *J. Biochem.* **1997**, *121*, 974.
23. Willenbrock, F.; Brocklehurst, K. *Biochem. J.* **1985**, *227*, 521.
24. Schechter, I.; Berger, A. *Biochem. Biophys. Res. Commun.* **2012**, *425*, 497.

25. Watanabe, D.; Yamamoto, A.; Tomoo, K.; Matsumoto, K.; Murata, M.; Kitamura, K.; Ishida, T. *J. Mol. Biol.* **2006**, *362*, 979.
26. Towatari, T.; Nikawa, T.; Murata, M.; Yokoo, C.; Tamai, M.; Hanada, K.; Katunuma, N. *FEBS Lett.* **1991**, *280*, 311.
27. Schaschke, N.; Assfalg-Machleidt, I.; Machleidt, W.; Turk, D.; Moroder, L. *Bioorg. Med. Chem.* **1997**, *5*, 1789.
28. Schaschke, N.; Assfalg-Machleidt, I.; Machleidt, W.; Moroder, L. *FEBS Lett.* **1998**, *421*, 80.
29. Katunuma, N.; Matsui, A.; Inubushi, T.; Murata, E.; Kakegawa, H.; Ohba, Y.; Turk, D.; Turk, V.; Tada, Y.; Asao, T. *Biochem. Biophys. Res. Commun.* **2000**, *267*, 850.
30. Katunuma, N.; Murata, E.; Kakegawa, H.; Matsui, A.; Tsuzuki, H.; Tsuge, H.; Turk, D.; Turk, V.; Fukushima, M.; Tada, Y.; Asao, T. *FEBS Lett.* **1999**, *458*, 6.
31. Singh, J.; Petter, R. C.; Baillie, T. A.; Whitty, A. *Nat. Rev. Drug Disc.* **2011**, *10*, 307.
32. Kitz, R.; Wilson, I. B. *J. Biol. Chem.* **1962**, *237*, 3245.
33. Knight, C. G. *Biochem. J.* **1980**, *189*, 447.
34. Kumar, S.; Zhou, B.; Liang, F.; Wang, W. Q.; Huang, Z.; Zhang, Z. Y. *Proc. Natl. Acad. Sci. U.S.A.* **2004**, *101*, 7943.
35. Brandl, M.; Weiss, M. S.; Jabs, A.; Suhnel, J.; Hilgenfeld, R. *J. Mol. Biol.* **2001**, *307*, 357.
36. Mort, J. S. Handbook of Proteolytic Enzymes In Barret, A. J., Rawlings, N. D., Woessner, J. F., Jr., Eds., 2nd ed.; Elsevier: UK, 2004; p 1079.
37. Aronson, N. N., Jr.; Barrett, A. J. *Biochem. J.* **1978**, *171*, 759.
38. Takahashi, T.; Dehdarani, A. H.; Yonezawa, S.; Tang, J. *J. Biol. Chem.* **1986**, *261*, 9375.
39. Dana, D.; Das, T. K.; Kumar, I.; Davalos, A. R.; Mark, K. J.; Ramai, D.; Chang, E. J.; Talele, T. T.; Kumar, S. *Chem. Biol. Drug Des.* **2012**, *80*, 489.
40. Mohamed, M. M.; Sloane, B. F. *Nat. Rev. Cancer* **2006**, *6*, 764.
41. Abudula, A.; Rommerskirch, W.; Weber, E.; Gunther, D.; Wiederanders, B. *Biol. Chem.* **2001**, *382*, 1583.
42. Muntener, K.; Zwicky, R.; Csucs, G.; Rohrer, J.; Baici, A. *J. Biol. Chem.* **2004**, *279*, 41012.
43. Szpaderska, A. M.; Silberman, S.; Ahmed, Y.; Frankfater, A. *Anticancer Res.* **2004**, *24*, 3887.
44. Sameni, M.; Moin, K.; Sloane, B. F. *Neoplasia* **2000**, *2*, 496.
45. Krepela, E.; Vicar, J.; Cernoch, M. *Neoplasma* **1989**, *36*, 41.
46. Baricos, W. H.; Zhou, Y.; Mason, R. W.; Barrett, A. J. *Biochem. J.* **1988**, *252*, 301.
47. Hulkower, K. I.; Butler, C. C.; Linebaugh, B. E.; Klaus, J. L.; Keppler, D.; Giranda, V. L.; Sloane, B. F. *Eur. J. Biochem/FEBS* **2000**, *267*, 4165.
48. Handschuh, G.; Candidus, S.; Luber, B.; Reich, U.; Schott, C.; Oswald, S.; Becke, H.; Hutzler, P.; Birchmeier, W.; Hofler, H.; Becker, K. F. *Oncogene* **1999**, *18*, 4301.
49. Chao, Y. L.; Shepard, C. R.; Wells, A. *Mol. Cancer* **2010**, *9*, 179.
50. Wang, F.; Hansen, R. K.; Radisky, D.; Yoneda, T.; Barcellos-Hoff, M. H.; Petersen, O. W.; Turley, E. A.; Bissell, M. J. *J. Natl Cancer Inst.* **2002**, *94*, 1494.
51. Onder, T. T.; Gupta, P. B.; Mani, S. A.; Yang, J.; Lander, E. S.; Weinberg, R. A. *Cancer Res.* **2008**, *68*, 3645.
52. Stemmler, M. P. *Mol. BioSyst.* **2008**, *4*, 835.
53. Paredes, J.; Figueiredo, J.; Albergaria, A.; Oliveira, P.; Carvalho, J.; Ribeiro, A. S.; Caldeira, J.; Costa, A. M.; Simoes-Correia, J.; Oliveira, M. J.; Pinheiro, H.; Pinho, S. S.; Mateus, R.; Reis, C. A.; Leite, M.; Fernandes, M. S.; Schmitt, F.; Carneiro, F.; Figueiredo, C.; Oliveira, C.; Seruca, R. *Biochim. Biophys. Acta* **2012**, *1826*, 297.
54. Wong, A. S.; Gumbiner, B. M. *J. Cell Biol.* **2003**, *161*, 1191.
55. Nollet, F.; Berx, G.; van Roy, F. *Mol. Cell Biol. Res. Commun.* **1999**, *2*, 77.
56. Schmidt, C. R.; Gi, Y. J.; Patel, T. A.; Coffey, R. J.; Beauchamp, R. D.; Pearson, A. S. *Surgery* **2005**, *138*, 306.
57. Li, L.; Hartley, R.; Reiss, B.; Sun, Y.; Pu, J.; Wu, D.; Lin, F.; Hoang, T.; Yamada, S.; Jiang, J.; Zhao, M. *Cell. Mol. Life Sci.* **2012**, *69*, 2779.
58. Desai, R. A.; Gao, L.; Raghavan, S.; Liu, W. F.; Chen, C. S. *J. Cell Sci.* **2009**, *122*, 905.
59. Arai, S.; Shioiri, T. *Tetrahedron* **2002**, *58*, 1407.
60. Brown, S.; Bernardo, M. M.; Li, Z. H.; Kotra, L. P.; Tanaka, Y.; Fridman, R.; Mobashery, S. *J. Am. Chem. Soc.* **2000**, *122*, 6799.
61. Eisch, J. J.; Galle, J. E. *J. Org. Chem.* **1979**, *44*, 3277.
62. Lee, M.; Ikejiri, M.; Klimpel, D.; Toth, M.; Espahbodi, M.; Hesek, D.; Forbes, C.; Kumarasiri, M.; Noll, B. C.; Chang, M.; Mobashery, S. *ACS Med. Chem. Lett.* **2012**, *3*, 490.
63. Moin, K.; Day, N. A.; Sameni, M.; Hasnain, S.; Hirama, T.; Sloane, B. F. *Biochem. J.* **1992**, *285*(Pt 2), 427.
64. Turk, B.; Dolenc, I.; Zerovnik, E.; Turk, D.; Gubensek, F.; Turk, V. *Biochemistry* **1994**, *33*, 14800.
65. Abdo, M.; Liu, S.; Zhou, B.; Walls, C. D.; Wu, L.; Knapp, S.; Zhang, Z. Y. *J. Am. Chem. Soc.* **2008**, *130*, 13196.
66. Wang, B.; Shi, G. P.; Yao, P. M.; Li, Z.; Chapman, H. A.; Bromme, D. *J. Biol. Chem.* **1998**, *273*, 32000.
67. Kirschke, H.; Wiederanders, B. *Methods Enzymol.* **1994**, *244*, 500.
68. Tavares, F. X.; Boncek, V.; Deaton, D. N.; Hassell, A. M.; Long, S. T.; Miller, A. B.; Payne, A. A.; Miller, L. R.; Shewchuk, L. M.; Wells-Knecht, K.; Willard, D. H., Jr.; Wright, L. L.; Zhou, H. Q. *J. Med. Chem.* **2004**, *47*, 588.
69. Nakajima, K.; Powers, J. C.; Ashe, B. M.; Zimmerman, M. *J. Biol. Chem.* **1979**, *254*, 4027.
70. Walsh, K. A. *Methods Enzymol.* **2012**, *19*, 41.
71. Cadene, M.; Chait, B. T. *Anal. Chem.* **2000**, *72*, 5655.
72. Fenyo, D.; Wang, Q.; DeGrasse, J. A.; Padovan, J. C.; Cadene, M.; Chait, B. T. *J. Vis. Exp.* **2007**, 192.
73. Abeyweera, T. P.; Chen, X.; Rotenberg, S. A. *J. Biol. Chem.* **2009**, *284*, 17648.
74. Salaycik, K. J.; Fagerstrom, C. J.; Murthy, K.; Tulu, U. S.; Wadsworth, P. *J. Cell Sci.* **2005**, *118*, 4113.
75. Fabre-Guillevin, E.; Malo, M.; Cartier-Michaud, A.; Peinado, H.; Moreno-Bueno, G.; Vallee, B.; Lawrence, D. A.; Palacios, J.; Cano, A.; Barlovatz-Meimon, G.; Charriere-Bertrand, C. *Breast Cancer Res.* **2008**, *10*, R100.
76. Chen, X.; Zhao, X.; Abeyweera, T. P.; Rotenberg, S. A. *Biochemistry* **2012**, *51*, 7087.